Statistical analysis of neutrino-induced hadron production from a different perspective

Rashi Sharma[*]
Department of Physics, Syracuse University, Syracuse, New York 13244, USA

R. Aggarwal[†]
USAR, Guru Gobind Singh Indraprastha University, East Delhi Campus, 110092, India

M. Kaur[‡]
Department of Physics, Panjab University, Chandigarh 160014, India and Department of Physics, Amity University, Punjab, Mohali 140306, India

(Received 2 August 2023; accepted 8 December 2023; published 29 December 2023)

With four different type of neutrino-induced interactions, we investigate and reanalyze the Koba-Nielsen-Olesen scaling in modified multiplicity distributions from a different perspective. In a first of its kind attempt, we propose alternate fitting function to parametrize the distribution than the most widely adopted Slattery's function and compare it with yet another form. We propose the shifted Gompertz and Weibull functions as the fitting functions and compare their potency for the most conventional form of Slattery's function. In addition, the analysis of the data by evaluating the central moments and factorial moments, we show the dependence of moments on the target size.

DOI: 10.1103/PhysRevD.108.113011

I. INTRODUCTION

The study of multiplicity distributions of charged hadrons produced in lepton-induced and hadron-induced interactions in different targets has remained in focus ever since the advent of high energy and cosmic ray physics. It has been extensively studied in fixed-target and collider experiments as well as in cosmic ray experiments. The results of such studies are utilized in modeling of interaction dynamics. In contrast to the vast information available from experiments using leptons and hadrons as probes, accessibility of such information from neutrino-induced experiments has remained very limited. Earliest studies on the charged hadronic multiplicities in charged-current (CC) and neutral-current (NC) interactions measured in experiments performed with 15-foot bubble chamber during 1970s to the latest results from the OPERA experiment using CERN CNGS neutrino beams, and the CHORUS experiment have provided results in different center-of-mass (cms) energies and in different phase space regions [1–5]. The mean charged-hadron multiplicities in the muon-neutrino and muon-antineutrino charged-current reactions on hydrogen and deuterium have been measured in the Fermilab experiments E31 [6,7], E45 [8,9] and E-545 [10,11] with the 15-foot Bubble Chamber and in the CERN experiments WA21 [12,13] and WA25 [14,15] with the Big European Bubble Chamber (BEBC). The data obtained with the FNAL and BNL hydrogen bubble chambers before 1976 are gathered in Ref. [16]. The motivation for the present study stems from the fact that there is one common investigation which has been performed on the data from all these experiments. It relates to the study of Koba-Nielsen-Olesen (KNO) scaling [17,18], a study which provides understanding of improving models of particle production which are used in Monte Carlo (MC) event generators. There are many neutrino-nucleon and neutrino-nucleus event generators such as, NEUGEN [19,20], FLUKA [21], GENIE [22], NuWro [23], GiBUU [24], and NUANCE [25] etc. The next generation detectors like the DUNE [26] and Super-Kamiokande [27] which aim at understanding the role of neutrinos in the universe, are primarily focused on collecting the neutrino interaction data in the not too far future, rely on the MC event generators. The region of interaction kinematics proposed for study in these experiments have neutrino energies in the few GeV range. The investigation presented in this paper have average neutrino energies

[*]rsharm18@syr.edu
[†]ritu.aggarwal1@gmail.com
[‡]manjit@pu.ac.in

in >10–50 GeV. Hence the study is relevant for comparison with the data from these future experiments. The major challenge with any event generator which remains, is to tune it's model parameters to the recorded experimental data. The event multiplicity data mimic the underlying event mechanism and are extensively used to tune the model parameters. The neutrino experiments have large errors associated with them due to small sample sizes. A precise analysis of the existing data can contribute to MC development.

KNO scaling derived from Feynman scaling showed that total multiplicity undergoes asymptotic scaling at high energies as the average charged multiplicity, $\langle n_{\rm ch}\rangle \propto \ln\sqrt{s}$. The KNO formalism is described in detail in Sec. II. In almost all the results on KNO distributions, different experiments using neutrino beams have used the Slattery's function in different forms, to fit the KNO distributions [1,5,11]. However, the multiplicity data on neutrino interactions are very rare. Only recently, two emulsion based neutrino experiments OPERA and CHORUS [1,5] published multiplicity distributions and also tested KNO scaling with a reliable statistics. The multiplicity distribution for each data follows a negative binomial distribution exhibiting approximate KNO scaling. The KNO scaled distribution has been described with the Slattery's function. The aim of the present work is to show that the KNO distribution can be defined in terms of different functions with improved precision than the Slattery's function. A comparison of two different distributions, namely the shifted Gompertz and the Weibull distributions with the Slattery's distribution is presented. In addition we also evaluate central and factorial moments of the multiplicity distributions, both from the data and the best fitted proposed distribution. With four type of neutrino interactions considered, we set out to study the effect of KNO scaling in their multiplicity distributions. Two new fitting functions are proposed and their potency for all the above cases is studied.

One of the consequences of the KNO scaling is that the dispersion over mean multiplicity is rendered independent of kinematic quantities. The probability distribution of n-particle events is also well represented by the moments of the distribution and its generating function. The analysis of multiplicity moments is a powerful tool which helps to unfold the characteristics of the multiplicity distribution. Calculated as derivatives of the generating function, the particle correlations can be studied through the normalized central moments. Dependence of moments on energy can be used to validate the KNO scaling [28,29] or to check for violation. Several analyses of multiplicity moments have been done at various energies, using different probability distribution functions [30–34]. However, these analyses mostly are done for e^+e^-, pp and $\bar{p}p$ collisions. Such studies in neutrino-induced interactions are missing. The presented work is the first analysis using new distributions for the case of ν-X and $\bar{\nu}$-X interactions, where X is a target.

II. METHODOLOGY

The multiplicity distribution is expressed in terms of the probability of producing n number of particles in the final state of a collision. The shape of such a distribution varies with system size and collision energy and can be incorporated into the study of its higher moments. The multiplicity distribution of charged hadrons produced in the neutrino interactions reflects the characteristics of hadronic final states in hard scattering. These type of data assist to improve models of particle production which are used in Monte Carlo (MC) event generators. The shape of the multiplicity distribution is often studied in terms of functional dependence of the probability on the number of particles n, produced in a collision. The following sections describe various forms most commonly used and the new proposed functions.

A. KNO formalism

Koba, Nielsen, and Olesen showed that when the multiplicity distributions were scaled by average multiplicity $\langle n_{ch}\rangle$, they became asymptotically independent of the energy of interaction. The KNO hypothesis shows that at very high center-of-mass (CMS) energy $\sqrt{s}$, the probability P_n of producing n charged particles in a collision process having the mean number of charged particles $\langle n\rangle$, should follow the following scaling relation:

$$P_n(s) = \frac{1}{\langle n\rangle}\psi(z,s) = \lim_{s\to\infty}\frac{1}{\langle n\rangle}\psi(z), \quad \text{where } z = \frac{n}{\langle n\rangle}, \tag{1}$$

Thus, the data points $P_n(s)$ measured at different energies $\sqrt{s}$, should fall on a single curve defined by the function ψ. This curve can then be parametrized by fitting a function.

B. Parametrization of KNO distributions

Parametrization of the KNO scaled distributions was first introduced by Slattery (SL) [35] in the form

$$\psi(z) = (A_1 z^3 + B_1 z^4)e^{-C_1 z} \tag{2}$$

Various experiments [1,5,11] used this form to fit the KNO distributions. The data from the experiments involving neutrino interactions show that approximate KNO scaling as a function of an appropriate multiplicity variable $z\prime$ is valid for the charged hadrons multiplicity. However, the interaction energies are typically low, with W^2 of the order of 35 GeV^2. For ν_μ charged-current (CC) interactions,

$$W^2 = 2m_N E_{\rm had} + m_N^2 - Q_\nu^2, \tag{3}$$

where Q_ν^2 is the squared four-momentum transfer, and m_N is the nucleon mass. W^2 is the square of the invariant mass of the hadronic system. The first observation of the KNO violation came from pp interactions at the Intersecting

Storage Ring (ISR). The violation was soon discovered at other energies and in other interactions involving e^+e^-, $p\bar{p}$ etc. KNO scaling violation led to the application of negative binomial distribution (NBD), introduced by P. Carruthers *et al.* [36,37].

With a low priority of using KNO scaled distributions, different experiments used NBD to unwind the mechanism of particle production. The success of NBD was phenomenal in providing a description in a most consistent way. Over a period of time, some more statistical distributions were introduced and used for interpreting the data. These include gamma distribution [38], lognormal distribution [39], Tsallis distribution [40,41], and the more recent Weibull distribution (Wei) [42,43]. Nevertheless, at very high energies, typically in the TeV range, NBD was also seen to deviate.

In the present work we introduce a yet novel way to parametrize the KNO distribution and show that its agreement is far improved in comparison to the Slattery's function. We choose shifted Gompertz distribution (SGD) to fit the KNO scaled distributions and compare it with Slattery's function and the Weibull distribution. A description of this new distribution follows in the next section.

C. The shifted Gompertz distribution (SGD)

In one of our earlier works, we put in place the use of shifted Gompertz distribution [44], first introduced by [45], to investigate the multiplicities in leptonic and hadronic collisions for different collision energies. The distribution interpreted the experimental data from high-energy particle collisions involving leptons and hadrons as probes, very well.

The SGD distribution uses two non-negative parameters; one of them is known as the scale parameter and the other a shape parameter. Taking these parameters as $b > 0$ and $t > 0$, the probability density function of a variable n is then defined as

$$P_n = be^{-bn}e^{-(te^{-bn})}[1 + t(1 - e^{-bn})]n > 0, \qquad (4)$$

Maximum of two independent random variables with Gompertz distribution (parameters $b > 0$ and $t > 0$) and an exponential distribution (parameter $b > 0$), characterize the distribution. We used SGD in describing multiplicity data in e^+e^-, e^+p, pp, $\bar{p}p$ data at different energies and showed that SGD provides a good description [44,46–48].

D. The Weibull distribution (Wei)

A highly versatile probability density function (pdf), the Weibull distribution [49] can fit a wide range continuous data. It has been used to study the data from different regimes such as medicine, quality control, engineering etc. and can also be used to model the skewed data quite well. The probability density function of this distribution is expressed in three different forms; 3-parameter Weibull, 2-parameter Weibull, and 1-parameter Weibull.

The 3-parameter Weibull probability density function is given by

$$P_n = \frac{\beta}{\eta}\left(\frac{n-\gamma}{\eta}\right)^{\beta-1} e^{-\left(\frac{n-\gamma}{\eta}\right)^{\beta}} \qquad (5)$$

where $P_n \geq 0$, $n > \gamma$, where γ is the location parameter and $-\infty < \gamma < +\infty$. The shape parameter $\beta > 0$ and the scale parameter $\eta > 0$. By setting $\gamma = 0$, one gets the 2-parameter Weibull pdf

$$P_n = \frac{\beta}{\eta}\left(\frac{n}{\eta}\right)^{\beta-1} e^{-\left(\frac{n}{\eta}\right)^{\beta}} \qquad (6)$$

The 1-parameter Weibull assumes the only unknown as the scale parameter η, the shape parameter β is known *a priori* and hence a constant, with Eq. (6) is used and compared with results from SGD.

E. Moments of multiplicity distribution

The moments are calculated as derivatives of the generating function and the particle correlations can be studied through the normalized moments (C_q) and normalized factorial moments (F_q) which are defined as [50];

$$C_q = \frac{\langle n^q \rangle}{\langle n \rangle^q} = \frac{\sum_n n^q P_n}{(\sum_n n P_n)^q} \qquad (7)$$

$$F_q = \frac{\sum_{n=q}^{n_{\max}} n(n-1).....(n-q+1)P_n}{(\sum_{n=1}^{n_{\max}} nP_n)^q} \qquad (8)$$

F. Trends in mean multiplicity dependence on W^2

In order to compare the dependency of average charged hadron multiplicity on the invariant mass of hadronic system, the data from different experiments are studied. The invariant hadronic mass is expressed as in Eq. (3). The mean charged hadron multiplicity is found to vary linearly as a function of logarithm of the square of the invariant mass of the hadronic system W, in various ranges of W^2,

$$\langle n_{ch} \rangle = a + b(lnW^2) \qquad (9)$$

This linear variation was found to be true for all energies.

G. Dispersion trends

Dispersion $D\left(= \sqrt{\langle n_{ch}^2 \rangle - \langle n_{ch} \rangle^2}\right)$ of multiplicity distribution of n particles is interesting from theoretical point of view. It is understood that for independent particle emission, the dispersion versus average multiplicity should follow a Poisson distribution. However, it is observed that in hadronic interactions the variation of dispersion follows an empirical relation with multiplicity as;

$$D = A + B\langle n_{ch} \rangle \qquad (10)$$

For data from different experiments, we study this dependence. The interpolation of the fit from Eq. (10) gives an unexpected intercept at the $\langle n_{ch} \rangle$ axis. The value of the intercept is used to modify the KNO distribution for improving fitting with different functions.

III. DATA ANALYZED

Data from the four major experiments have been analyzed with details as given below.

A. Data from the OPERA experiment

The OPERA experiment was designed to observe and study the neutrino oscillations in the $\nu_\mu \to \nu_\tau$ oscillations in appearance mode in the CNGS (CERN Neutrinos to Gran Sasso) neutrino beam [51,52]. The experiment established neutrino oscillations with the discovery of ν_τ appearance with a significance of 5.1σ [1]. The OPERA detector was a hybrid setup consisting of electronic detectors and a massive lead-emulsion target. The nuclear emulsions were used as very precise tracking devices and electronic detectors to locate the neutrino interaction events in the emulsions. It was exposed to the CNGS ν_μ beam with mean energy of 17 GeV. A data sample corresponding to 1.8×10^{20} protons on target (p. o.t.) collected during the period 2008 to 2012 as published in [52]), the electronic detectors recorded 19505 neutrino interactions in the target fiducial volume. A subsample of 818 events occurring in the lead with a negatively charged muon was selected in order to measure the track and vertex parameters in the target including a detailed check of the nuclear breakup and evaporation processes. Imposing an additional requirement of selecting events with $W^2 > 1$ GeV^2 to eliminate quasielastic events, a total of 795 events were selected. Description of the OPERA detector and selection procedures can be found in [52].

In the present analysis, we have used the charged hadron multiplicities obtained from 795 ν_μ-Pb events in different W^2 ranges and corrected for efficiencies from the papers by N. Agafonova *et al.* [1–3]. In Ref. [1], the charged hadron multiplicity as a function of W^2 from Table III and the efficiency corrections from Table II have been used to reproduce the multiplicity distribution being used in the present analysis.

B. Data from the CHORUS experiment

The CHORUS experiment was designed to search for $\nu_\mu \to \nu_\tau$ oscillations. The CHORUS hybrid detector was exposed to the wide band neutrino beam of the CERN SPS during the years 1994–1997, with an integrated flux of 5.06×10^{19} protons on nuclear emulsion target. The West Area Neutrino Facility (WANF) of the CERN SPS provided an intense beam of neutrinos with an average energy of 27 GeV. More than 10^6 neutrino interactions were accumulated in the emulsion target. A requirement on the square of the invariant mass of the hadronic system, $W^2 > 1$ GeV^2 along with other selection criteria to remove the background, was imposed. A sample of 496 ν_μ-A and 369 $\bar{\nu}_\mu$-A events, where A represents the target, was finally selected for analysis. Details of the data as number of events for every W^2 range can be obtained from Ref. [5]. Investigation into the KNO scaling [17] behavior of the charged hadron multiplicity in different kinematical regions has been done. Using the multiplicity distributions thus obtained for both ν-A and $\bar{\nu}$-A are analyzed to validate the mean multiplicity values cited in Tables 5 and 6 of Ref. [5] and used for further analysis in the present work.

C. νn and νp charged-current interactions from Fermilab Bubble Chamber

Charged-hadron multiplicity distributions in νn and νp charged-current (CC) interactions were measured in an exposure of the Fermilab deuterium-filled 15-foot bubble chamber to a wide-band neutrino beam produced by 350-GeV protons. Charged-hadron multiplicities initiated in charged-current neutrino interactions on deuteron targets, from which νn and νp collisions from an identical neutrino flux were separated. The data sample corresponds to a flux of 4.57×10^{18} protons on target. The average neutrino energy was 50 GeV.

$$\begin{aligned} &\nu_\mu + n \to \mu^- + X^+, \qquad X^+ \to \text{hadrons} \\ &\nu_\mu + p \to \mu^- + X^{++}, \qquad X^{++} \to \text{hadrons} \end{aligned} \tag{11}$$

Charged hadron multiplicity distributions published in [11] measured for (a) 9237 neutrino-neutron CC interactions and (b) 6033 neutrino-proton CC interactions, distributed over different W^2 ranges between 1-225 GeV^2 are used for the present analysis. The paper by D. Zieminska *et al.* [11], contains details of the data and selection procedure used.

D. νp charged current interactions from Fermilab Bubble Chamber

The multiplicity distributions of the hadrons produced in antineutrino-proton interactions in a sample consisting of 2055 ± 206 charged-current events with antineutrino energy greater than 5 GeV are analyzed using the data from reference [7]. The data comes from exposures of the 15-foot hydrogen bubble chamber to the broad-band antineutrino beam at Fermilab. The distribution in hadronic mass W has an average value of 3.7 GeV but extends up to 10 GeV. The data samples were obtained from three separate exposures of the Fermilab 15-foot hydrogen bubble chamber. The events were obtained with a 400 GeV proton beam incident on an aluminium target. Two horns were used to focus the produced negative particles which in turn decayed to generate the $\bar{\nu}_\mu$ beam. The $\bar{\nu}p$ charged-current (CC) events were extracted from

the sample that included contributions from both CC and NC reactions.

$$\bar{\nu}p \to \mu^+ H^0,$$
$$\nu p \to \mu^- H^{++},$$
$$\bar{\nu}p \to \bar{\nu} H^+,$$
$$\nu p \to \nu H^+$$

The bulk of the charged-current data are in the W range, $2 < W < 6$ GeV with a median W value of 3.7 GeV. The details of the data for every W range can be obtained from Ref. [7].

The data samples discussed above have different neutrino energies and different target size (A). The target size is related to the mean number of inelastic collisions and hence the $\langle n_{ch} \rangle$. In the production process, the main interest is to study the inelastic interactions. However, not all events are deep inelastic, some have very low Q^2 and the multiplicity dependence is not linear with respect to the target size as discussed in Ref. [53] for the case of hadron-nucleon and hadron-nucleus case. In the present analysis, all data samples under study have $Q^2 \geq 5$ GeV^2 and the $\langle E_\nu \rangle > 10$ GeV.

IV. RESULTS

Figure 1 shows the dependence of $\langle n_{ch} \rangle$ on $\ln W^2$ for each specified data being analyzed. Most of the earlier studies made a linear fit, $\langle n_{\rm ch} \rangle = a + b \ln W^2$ to each dataset. Accordingly a linear fit has been made to validate the data used, and the values of parameters a and b as shown in Table I are found to be very close to the earlier results.

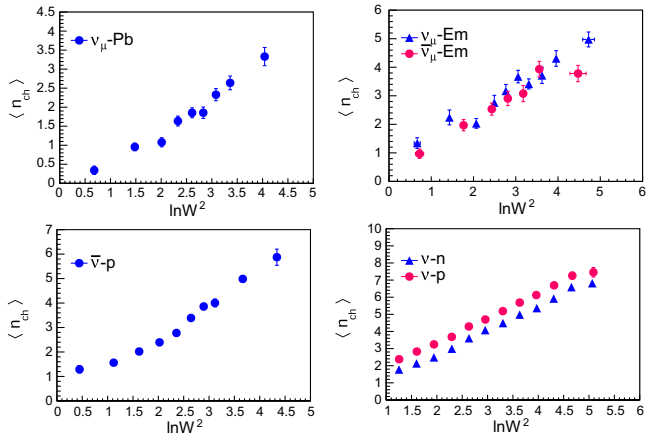

FIG. 1. Average charged hadron multiplicity $\langle n_{ch} \rangle$ as a function of $\ln W^2$. The data on interactions (i) ν_μ-Pb collected by the OPERA experiment using CERN-CNGS [1] (ii) ν_μ-Em and $\bar{\nu}_\mu$-Em by the CHORUS experiment [5] (iii) $\bar{\nu}$-p using FNAL-Bubble Chamber [7] (iv) ν-n and ν-p obtained from FNAL-Bubble Chamber [11].

TABLE I. Linear fit parameters for $\langle n_{\rm ch} \rangle$ versus $\ln W^2$ dependence.

Interaction	A	B	χ^2/ndf	Reference
ν_μ-Pb	-0.27 ± 0.06	0.81 ± 0.03	22.55/7	[1]
ν_μ-Em	0.69 ± 0.18	0.87 ± 0.06	11.8/8	[5]
$\bar{\nu}_\mu$-Em	0.48 ± 0.18	0.84 ± 0.07	5.03/5	[5]
$\bar{\nu}$ p	-0.40 ± 0.12	1.43 ± 0.05	12.6/6	[7]
ν n	-0.19 ± 0.06	1.42 ± 0.02	14.4/9	[11]
ν p	0.49 ± 0.13	1.43 ± 0.05	2.26/9	[11]

Figure 2 shows the dependence of dispersion D on the average multiplicity $\langle n_{\rm ch} \rangle$ for data on ν_μ-Pb interactions, from the OPERA experiment. A straight line fit equation (10) to the data confirms a linear dependence. The interpolation of the straight line fit on the $\langle n_{ch} \rangle$ axis is measured as a parameter, $\alpha = -\mathrm{A}/\mathrm{B}$. Similar linear dependencies are studied for all the datasets and the value of α obtained for each of the datasets. To avoid multiple similar figures, only one of these, is presented here. The fit coefficients A and B and the α values are shown in the Table II for all the datasets being analyzed. For all the distributions, the χ^2 minimization has been performed by using CERN software, the ROOT6.12.

A. Effect of α

KNO scaling as discussed in Sec. II was derived from Feynman scaling, observing that at high energy the KNO leads to an asymptotic scaling of the total multiplicity as $\langle n_{\rm ch} \rangle \propto \ln \sqrt{s}$. Thus, KNO scaling implies that the intercept A in Eq. (10) be compatible with 0, which is not the case at low to medium energies for all kinds of interactions. Alpha is calculated from Eq. (10) as $\alpha = -\mathrm{A}/\mathrm{B}$, a variable which is reaction independent but energy dependent. Using α, Buras *et al.* [54] provided an extension of the KNO scaling to low energies by introducing a new variable $z\prime$ defined as:

$$z\prime = \frac{n_{\rm ch} - \alpha}{\langle n_{\rm ch} - \alpha \rangle} \tag{12}$$

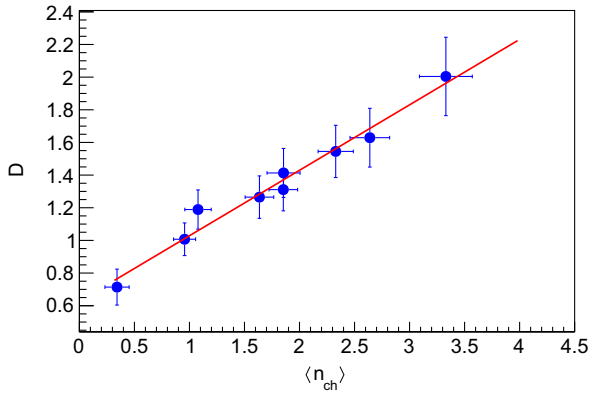

FIG. 2. Dispersion as a function of $\langle n_{\rm ch} \rangle$ for ν_μ-Pb interactions obtained by the OPERA experiment [1].

TABLE II. Dispersion D versus $\langle n_{ch}\rangle$ variation. Values of slope A, intercept B of the linear fit and the ratio $\alpha = -A/B$ are shown.

Interaction	A	B	χ^2/ndf	α	Reference
ν_μ-Pb	0.59 ± 0.05	0.42 ± 0.02	3.67/7	−1.410	[1]
ν_μ-Em	1.37 ± 0.23	0.14 ± 0.07	8.11/8	−6.468	[5]
$\bar{\nu}_\mu$-Em	1.14 ± 0.23	0.25 ± 0.09	1.51/5	−4.532	[5]
$\bar{\nu}$ p	0.54 ± 0.07	0.31 ± 0.03	2.39/8	−1.723	[7]
ν n	0.29 ± 0.04	0.36 ± 0.01	4.89/11	−0.928	[11]
ν p	0.09 ± 0.09	0.34 ± 0.02	2.26/9	−0.299	[11]

A possible explanation of α has been proposed in terms of a leading particle effect in interactions using hadrons, and neutrinos as well as resulting from the heavy nuclear targets in experiments using nuclear emulsions [5,54,55]. Figure 3 shows two KNO distributions for $\psi(z = \frac{n_{ch}}{\langle n_{ch}\rangle})$ and $\psi(z\prime = \frac{n_{ch}-\alpha}{\langle n_{ch}-\alpha\rangle})$ for the data from the OPERA experiment.

From the D versus $\langle n_{ch}\rangle$ linear fit, we get $\alpha = -1.41$. The distribution is fitted with the Slattery's function, Eq. (2), for two cases: (i) by including the α, and (ii) by taking $\alpha = 0$, to calculate $z\prime$. For both these cases, the distribution is also fitted with the shifted Gompertz function, Eq. (4) and the Weibull function, Eq. (6).

For the same data from the OPERA experiment, figure 3 shows the KNO distributions fitted with the Slattery's function, Eq. (2) for the two cases: (i) by including the α and (ii) by taking $\alpha = 0$, to calculate $z\prime$. The SGD and the Weibull distributions are also fitted.

From Table III it may be observed that χ^2/ndf falls by a large factor when including α to calculate $z\prime$. This shows a much improved performance of the fit functions in the description of the data, hence the justification to modify the variable z to $z\prime$. The same trend is observed for all the data under study.

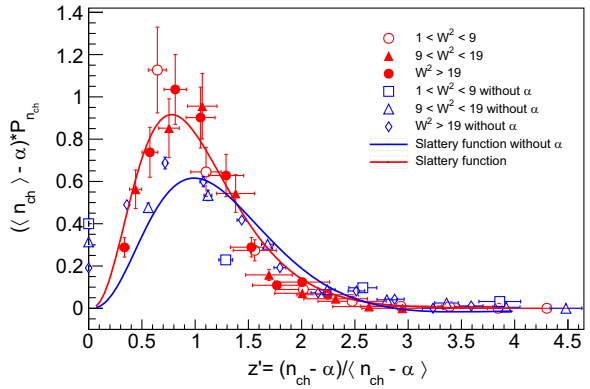

FIG. 3. KNO distributions for different W^2 (GeV^2) fitted with the Slattery's function (i) with $\alpha = 0$ (blue solid line) and (ii) with α included in the function (red solid line) for the data from the OPERA experiment [1].

TABLE III. KNO distribution fitted with different functions, with α, and with $\alpha = 0$ for the OPERA data [1].

Interaction	Distribution	$(\chi^2_\alpha$/ndf)	$(\chi^2_{\alpha=0}$/ndf)
ν_μ-Pb	SL	1.87	155.3
	SGD	0.39	33.41
	Wei	1.30	80.34

B. Different probability distribution functions

The KNO distribution has been studied by almost all the high energy physics experiments. For the case of neutrino interactions various forms of the Slattery's function [35] introduced in 1973, have been used to fit the distribution. Analysis of the data from the OPERA and the CHORUS experiments, used the function in the forms;

$$\psi(z\prime) = (Az\prime^3 + Bz\prime^4)e^{-Cz\prime} \tag{13}$$

$$\psi(z\prime) = (Az\prime + Bz\prime^3 - Cz\prime^5 + Dz\prime^7)e^{-Ez\prime} \tag{14}$$

where A, B, C, D, E are the fit parameters.

In Sec. II (B–D) we discussed the Slattery's function for KNO distribution, shifted Gompertz distribution and Weibull distributions. Details of the distributions are also provided. In the present work, we apply these distributions to investigate the KNO distributions with respect to the earlier used Slattery's function.

Figure 4 shows the KNO distribution for the ν_μ-Pb interactions in three W (GeV) ranges with $1 < W^2 < 9$, $9 < W^2 < 19$ and $W^2 > 19$ GeV^2 from the data obtained by the OPERA experiment [1].

Figures 5 and 6 show the KNO distributions for the ν_μ-Emulsion and $\bar{\nu}_\mu$-Emulsion interactions in two W (GeV) ranges with $1 < W^2 < 3$ and $3 < W^2 < 5$ GeV^2 for the data from the CHORUS experiment [5].

Figures 7 and 8 show the KNO distributions for the ν-n and ν-p interactions in five W(GeV) ranges with

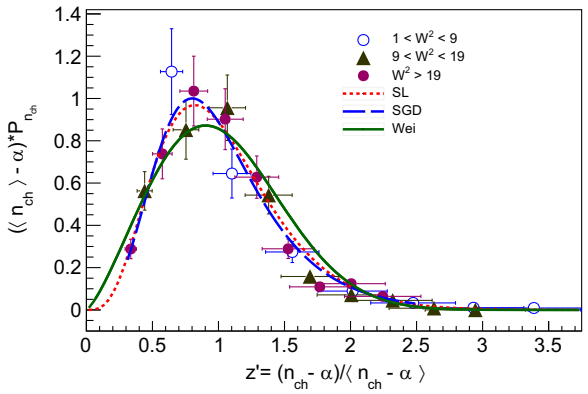

FIG. 4. KNO distributions of ν_μ-Pb data from the OPERA experiment [1], in different W (GeV) ranges, fitted with three different functions.

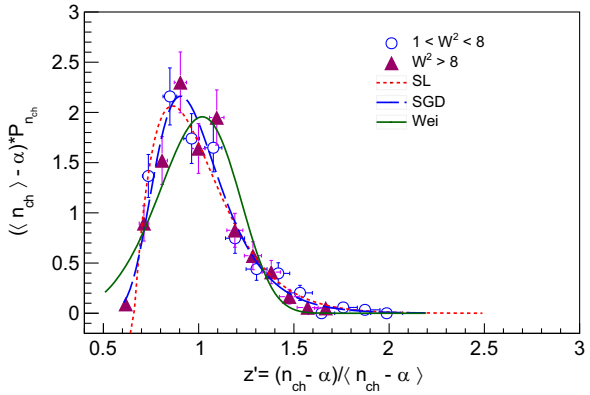

FIG. 5. KNO distributions of ν_μ-Emulsion data from the CHORUS experiment [5], in different $W(\mathrm{GeV})$ ranges, fitted with three different functions.

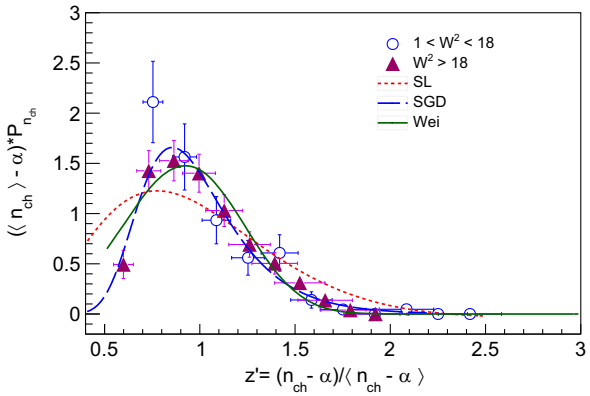

FIG. 6. KNO distributions of $\bar{\nu}_\mu$-Emulsion data from the CHORUS experiment [5], in different $W(\mathrm{GeV})$ ranges, fitted with three different functions.

$1 < W^2 < 3$, $3 < W^2 < 5$ and $5 < W^2 < 7$, $7 < W^2 < 10$ and $10 < W^2 < 15$ GeV^2 for the data from Ref. [11].

The KNO distributed data in Figs. 4–9 are fitted with three distributions: (i) Slattery's function, Eq. (13) (ii) shifted Gompertz function, Eq. (4), and (iii) the Weibull function, Eq. (6). Table IV shows the χ^2/ndf values for each of the fits and for each dataset. It is observed that the Slattery's function gives the maximum χ^2/ndf for every data, thereby showing it to be a bad fit. In Fig. 4 for the $\nu_\mu - \mathrm{Pb}$ data, SGD gives the best fit, closely followed by the Slattery's function. Weibull distribution however underestimates the data below $z' < 1$ and overestimates the data beyond $z' > 1$. Similar trend is found in the $\nu_\mu - \mathrm{Em}$ and $\bar{\nu} - \mathrm{n}$ interactions in Figs. 5 and 7. For the data presented in Figs. 6, 8, and 9, although the Weibull distribution behaves in the similar manner, the distribution due to Slattery's function in these cases, shows the worst fits, underestimates the data around the peak region and overestimate in the tail region. In all the cases peak value for Weibull distributions for all types of interaction, occurs at higher z', i.e., shifted to the right of the peak with respect

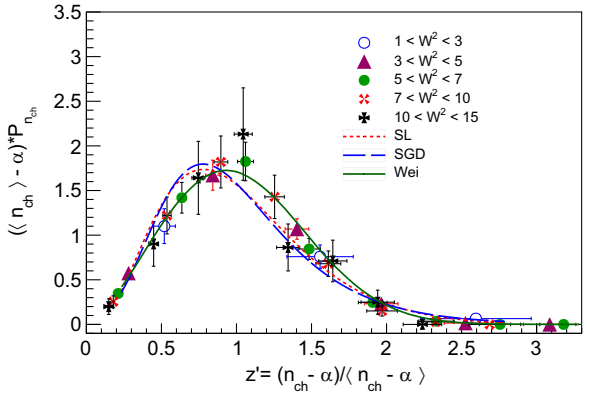

FIG. 7. KNO distributions of ν-n data from Ref. [11], in different $W(\mathrm{GeV})$ ranges, fitted with three different functions.

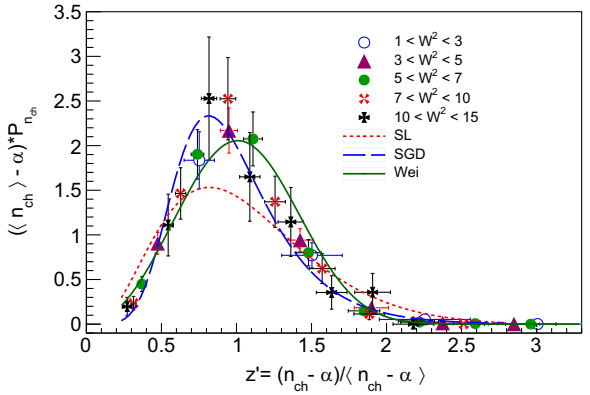

FIG. 8. KNO distributions of ν-p data from Ref. [11], in different $W(\mathrm{GeV})$ ranges, fitted with three different functions.

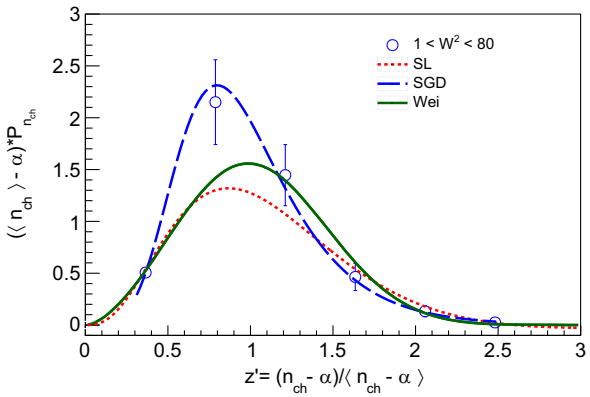

FIG. 9. KNO distributions of $\bar{\nu}$-proton data from Ref. [7] the with three different functions.

to both SGD and Slattery. The performance of the SGD turns out to be the best.

C. Central and factorial moments

Moment analysis is a powerful tool used for unfolding the characteristics of multiplicity distribution. The moments are

TABLE IV. Comparison of χ^2 values for the three functions: SL(Slattery's), SGD(shifted Gompertz), Wei(Weibull's) fitted to the data.

Interaction	$\langle W^2 \rangle$ GeV^2	SL χ^2/ndf	SGD χ^2/ndf	Wei χ^2/ndf	Reference
ν_μ-Pb	16.9 ± 0.6	1.87	0.40	1.30	[1]
ν_μ-Em	17.7 ± 0.8	0.85	0.52	2.72	[5]
$\bar{\nu}_\mu$-Em	26.2 ± 1.3	2.07	0.42	0.76	[5]
$\bar{\nu}$ p	28.62[a]	2.49	0.26	2.00	[7]
ν n	28.03[b]	0.71	0.93	0.27	[11]
ν p	29.41[b]	2.65	1.11	0.62	[11]

[a]Square of the quoted $\langle W \rangle$.
[b]The uncertainty in the determination of W due to ν-energy uncertainty is estimated to be 20% FWHM.

calculated as derivatives of the generating function of the probability distribution. Higher factorial moments from which all other kinds of moments, factorial moments can also be calculated and the particle correlations can be studied through them. The second central moment represents the variance of a random variable. It captures how spread out a distribution is. Higher variance means a wider distribution. The third moment called skewness, quantifies the relative size of the two tails of the distribution. Skewness is negative for longer left tails and positive for longer right tails. The third central moment is important because skewness is both location-and-scale-invariant. The fourth central moment represents kurtosis which is a measure of the combined size of the tails relative to whole distribution. In a logical manner higher moments, odd-powered central moments quantify relative tailedness and even-powered moments quantify total peakedness. Several analyses of moments have been done at different cms, using different probability distribution functions and variety of particles used as probes [30,32,34,56]. The higher moments also can identify the correlations among particles produced in collisions. Another study [57] on evolution of the multiplicity distribution in a fireball that cools down after chemical freeze-out focused on to obtain different apparent temperatures from different moments.

The values of central moments C_q and factorial moments F_q calculated for the experimental data and the SGD distributions which are the best fits of the data, are given in the Tables V and VI. Central moments are computed in terms of deviations from the mean, because then the higher-order central moments relate only to the spread and shape of the distribution. It may be observed that the normalized central moments as well as normalized factorial moments obtained from the shifted Gompertz distribution are in good agreement with the experimental values. This serves as a good test of the validity of the proposed SGD distribution. Additionally, it is also observed from the $\bar{\nu}(\nu)$-Emulsion interactions and $\bar{\nu}(\nu)$-proton interactions that all moments have higher values for the case of $\bar{\nu}$ interactions than the corresponding ν interactions with the same target. It is also observed that the values of both the central and factorial moments depend upon the target size A. Figures 10 and 11 and show the variation of C_2, C_3, C_4 moments derived from the experimental and SGD distributions. Similarly Figs. 12 and 13 show the variation of F_2, F_3, F_4 moments derived from the experimental and SGD distributions.

TABLE V. Normalized central moments C_q of experimental and shifted Gompertz distributions.

	Experimental				SGD				
Reaction	C_2	C_3	C_4	C_5	C_2	C_3	C_4	C_5	Reference
ν_μ-Pb	0.96 ± 0.06	1.17 ± 0.17	4.60 ± 0.61	14.21 ± 2.35	1.03 ± 0.05	1.50 ± 0.15	6.05 ± 0.61	21.04 ± 2.61	[1]
$\bar{\nu}$-Em	0.61 ± 0.23	0.31 ± 0.39	1.02 ± 0.83	1.31 ± 1.77	0.68 ± 0.07	0.48 ± 0.13	1.48 ± 0.31	2.45 ± 0.74	[5]
ν-Em	0.46 ± 0.15	0.21 ± 0.25	0.67 ± 0.51	0.85 ± 1.06	0.48 ± 0.04	0.31 ± 0.07	0.90 ± 0.15	1.40 ± 0.34	[5]
$\bar{\nu}$-p	0.40 ± 0.15	0.18 ± 0.26	0.58 ± 0.50	0.71 ± 1.05	0.42 ± 0.02	0.25 ± 0.03	0.74 ± 0.06	1.08 ± 0.13	[7]
ν-n	0.36 ± 0.09	0.17 ± 0.16	0.47 ± 0.28	0.64 ± 0.58	0.36 ± 0.01	0.21 ± 0.01	0.55 ± 0.03	0.83 ± 0.06	[11]
ν-p	0.24 ± 0.08	0.11 ± 0.13	0.23 ± 0.19	0.30 ± 0.35	0.24 ± 0.01	0.12 ± 0.01	0.25 ± 0.02	0.33 ± 0.03	[11]

TABLE VI. Normalized factorial moments F_q of experimental and shifted Gompertz distributions.

	Experimental				SGD				
Reaction	F_2	F_3	F_4	F_5	F_2	F_3	F_4	F_5	Reference
ν_μ-Pb	1.35 ± 0.09	2.19 ± 0.20	4.17 ± 0.46	8.37 ± 1.09	1.42 ± 0.07	2.62 ± 0.18	5.70 ± 0.48	13.36 ± 1.33	[1]
$\bar{\nu}$-Em	1.23 ± 0.48	1.59 ± 0.84	1.99 ± 1.35	2.28 ± 1.92	1.31 ± 0.13	1.84 ± 0.25	2.64 ± 0.44	3.57 ± 0.71	[5]
ν-Em	1.14 ± 0.38	1.40 ± 0.66	1.78 ± 1.10	2.25 ± 1.75	1.15 ± 0.09	1.54 ± 0.16	2.21 ± 0.29	3.20 ± 0.51	[5]
$\bar{\nu}$-p	1.06 ± 0.44	1.20 ± 0.67	1.43 ± 1.02	1.71 ± 1.50	1.08 ± 0.04	1.29 ± 0.07	1.71 ± 0.11	2.27 ± 0.17	[7]
ν-n	1.10 ± 0.29	1.32 ± 0.47	1.71 ± 0.79	2.32 ± 1.32	1.10 ± 0.02	1.35 ± 0.04	1.84 ± 0.07	2.69 ± 0.12	[11]
ν-p	1.02 ± 0.32	1.11 ± 0.48	1.30 ± 0.74	1.63 ± 1.16	1.02 ± 0.03	1.13 ± 0.04	1.37 ± 0.06	1.76 ± 0.09	[11]

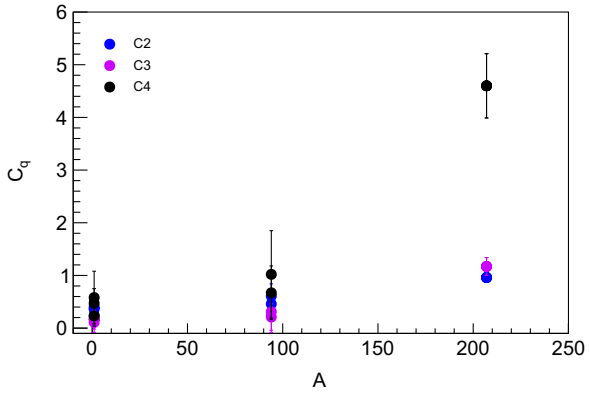

FIG. 10. Normalized central moments C_q as a function of the target mass A in ν-p ($A = 1$), ν-n ($A = 1$), ν_μ-Em ($A = 94$) and ν_μ-Pb($A = 207$) interactions, obtained from the data [1,5,11].

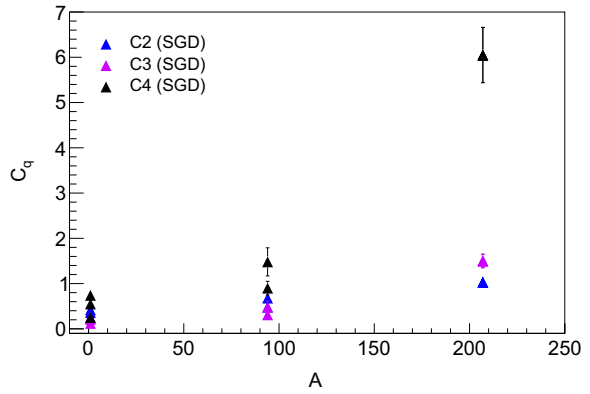

FIG. 11. Normalized central moments C_q as a function of the target mass A in ν-p ($A = 1$), ν-n ($A = 1$), ν_μ-Em ($A = 94$) and ν_μ-Pb($A = 207$) interactions, obtained from the SGD fit to the data [1,5,11].

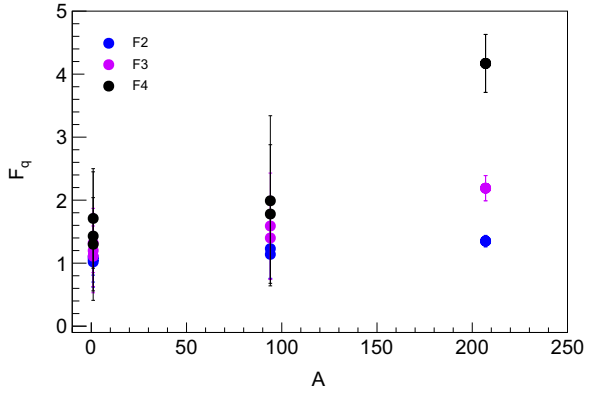

FIG. 12. Normalized factorial moments F_q as a function of the target mass A in ν-p ($A = 1$), ν-n ($A = 1$), ν_μ-Em ($A = 94$) and ν_μ-Pb($A = 207$) interactions, obtained from the data [1,5,11].

From these figures and the Tables V and VI it is found that the moments rise very fast for neutrino interactions with the target size; proton/neutron ($A = 1$) to Emulsion ($A = 94$) to Lead ($A = 207$).

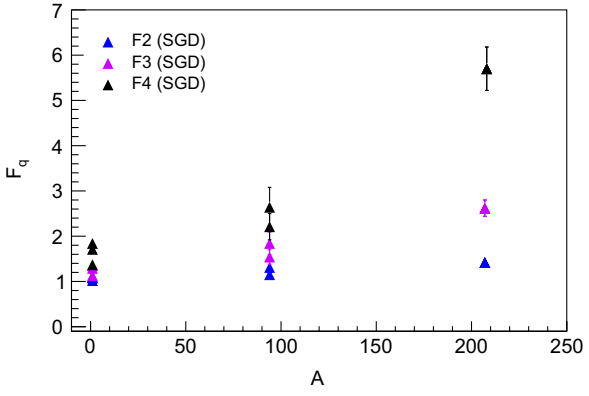

FIG. 13. Normalized factorial moments F_q as a function of the target mass A in ν-p ($A = 1$), ν-n ($A = 1$), ν_μ-Em ($A = 94$) and ν_μ-Pb($A = 207$) interactions, obtained from the SGD fit to the data [1,5,11].

V. CONCLUSION

A detailed analysis of the neutrino interactions has been done using data from four different experiments. This is the first study in which the KNO distribution is studied by using different functions than the conventional Slattery's function. The shifted Gompertz distribution and the Weibull distributions are studied. Both these distributions show a better agreement with the data in comparison to the Slattery's function. While the peak value of Slattery's function occurs around the same z' value as SGD, the peak for Weibull distribution is right-shifted. Both these distributions underestimate the hadron multiplicities below $z' < 1$ and overestimate beyond $z' > 1$, Slattery shows the worst fit, out of the two. However, the shifted Gompertz distribution shows the best agreement out of the three and hence SGD can serve as an estimator of hadron multiplicities while tuning the MC event generators for the future neutrino experiments.

The average multiplicity $\langle n_{ch} \rangle$ varies nearly linearly as a function of $\ln W^2$, although at very low W^2 it slightly departs. The dependence of the charged hadrons multiplicity on dispersion D also follows a linear relation equation (10).

It is interesting to observe that the values of both the central and factorial moments depend upon the target size A. Higher the atomic weight of the target, faster is the growth of the moments. Additionally, it is also observed from the $\bar{\nu}(\nu)$-Emulsion interactions and $\bar{\nu}(\nu)$-proton interactions that all moments have higher values for the case of ν interactions than the corresponding $\bar{\nu}$ interactions with the same target. A conclusive regularity in A-dependence can be studied if more number of data points with larger variation of target sizes becomes available. The information dissemination from such an analysis, particularly using the higher moments, is often useful to study the patterns and correlations.

ACKNOWLEDGMENTS

Authors R. S. and R. A. acknowledge the support of the Department of Technology, Savitribai Phule Pune University, India, where some of the work published here was undertaken under the DST INSPIRE Faculty grant.

[1] N. Agafonova *et al.*, Eur. Phys. J. C **78** (2018).
[2] N. Agafonova *et al.* (OPERA Collaboration), Phys. Rev. Lett. **115**, 121802 (2015).
[3] N. Agafonova *et al.* (OPERA Collaboration), Phys. Rev. Lett. **121**, 139901 (2018).
[4] K. S. Kuzmin and V. A. Naumov, Phys. Rev. C **88**, 065501 (2013).
[5] A. Kayis-Topaksu *et al.* (The CHORUS Collaboration), Eur. Phys. J. C **51**, 775 (2007).
[6] M. Derrick, P. Gregory, L. G. Hyman, K. Jaeger, D. Lissauer, R. J. Miller, B. Musgrave, J. J. Phelan, P. Schreiner, R. Singer, S. J. Barish, A. Engler, G. Keyes, T. Kikuchi, R. Kraemer, V. E. Barnes, D. D. Carmony, A. F. Garfinkel, and A. T. Laasanen, Phys. Rev. D **17**, 1 (1978).
[7] M. Derrick *et al.*, Phys. Rev. D **25**, 624 (1982).
[8] J. W. Chapman *et al.*, Phys. Rev. Lett. **36**, 124 (1976).
[9] J. Bell *et al.*, Phys. Rev. D **19**, 1 (1979).
[10] T. Kitagaki *et al.*, Phys. Lett. B **97**, 325 (1980).
[11] D. Zieminska *et al.*, Phys. Rev. D **27**, 47 (1983).
[12] G. Jones, R. Jones, D. Morrison, M. Mobayyen, S. Wainstein, M. Aderholz, D. Hantke, E. Hoffmann, U. Katz, J. Kern *et al.*, Z. Phys. C Part. Fields **46**, 25 (1990).
[13] G. Jones, R. Jones, D. Morrison, M. Mobayyen, S. Wainstein, M. Aderholz, D. Hantke, E. Hoffmann, U. Katz, J. Kern *et al.*, Z. Phys. C Part. Fields **54**, 45 (1992).
[14] D. Allasia *et al.*, Phys. Lett. B **135**, 231 (1984).
[15] D. Allasia, C. Angelini, A. Baldini *et al.* (WA25 Collaboration), Z. Phys. C **24**, 119 (1984).
[16] E. Albini, P. Capiluppi, G. Giacomelli, and A. M. Rossi, Nuovo Cimento Soc. Ital. Fis. **32A**, 101 (1976).
[17] Z. Koba, H. B. Nielsen, and P. Olesen, Nucl. Phys. **B40**, 317 (1972).
[18] M. Gazdzicki, R. Szwed, G. Wrochna, and A. K. Wroblewski, Mod. Phys. Lett. A **06**, 981 (1991).
[19] H. Gallagher, Nucl. Phys. B, Proc. Suppl. **112**, 188 (2002).
[20] H. R. Gallagher, in *Sixth international workshop on neutrino-nucleus interactions in the few-gev region nuint-09 sitges (barcelona), Spain* (American Institute of Physics, 2009), Vol. 1189, pp. 35–42, 10.1063/1.3274187.
[21] F. Ballarini *et al.*, J. Phys. Conf. Ser. **41**, 151 (2006).
[22] M. Kim (GENIE Collaboration), in Neutrino-nucleus interactions in the few-gev region: NuInt07: The 5th International Workshop on Neutrino-Nucleus Interactions in the Few-GeV Region (American Institute of Physics, 2007), Vol. **967**, pp. 310–312.
[23] J. Sobczyk, in *XXVIII International Conference on Neutrino Physics and Astrophysics* (2018), p. 353, 10.5281/zenodo.1301017.
[24] U. Mosel, J. Phys. G **46**, 113001 (2019).
[25] D. Casper, Nucl. Phys. B, Proc. Suppl. **112**, 161 (2002).
[26] B. Abi, R. Acciarri, M. A. Acero, G. Adamov *et al.*, J. Instrum. **15**, T08008 (2020).
[27] Y. Suzuki, Eur. Phys. J. C **79**, 298 (2019).
[28] R. E. Ansorge *et al.*, Z. Phys. C Part. Fields **43**, 357 (1989).
[29] G. Alner *et al.*, Phys. Lett. **160B**, 193 (1985).
[30] N. Suzuki, M. Biyajima, and N. Nakajima, Phys. Rev. D **54**, 3653 (1996).
[31] N. Nakajima, M. Biyajima, and N. Suzuki, Phys. Rev. D **54**, 4333 (1996).
[32] A. Capella, I. M. Dremin, V. A. Nechitailo, and J. T. T. Van, Z. Phys. C **75**, 89 (1996).
[33] M. Praszalowicz, Phys. Rev. Lett. **106**, 142002 (2011).
[34] A. K. Pandey, P. Sett, and S. Dash, Phys. Rev. D **96**, 074006 (2017).
[35] P. Slattery, Phys. Rev. D **7**, 2073 (1973).
[36] P. Carruthers and C. C. Shih, Int. J. Mod. Phys. A **02**, 1447 (1987).
[37] A. Giovannini and R. Ugoccioni, Int. J. Mod. Phys. A **20**, 3897 (2005).
[38] K. Urmossy, G. Barnaföldi, and T. Biró, Phys. Lett. B **718**, 125 (2012).
[39] R. Szwed, G. Wrochna, and A. K. Wróblewski, Mod. Phys. Lett. A **05**, 1851 (1990).
[40] C. Tsallis, J. Stat. Phys. **52**, 479 (1988).
[41] C. Aguiar and T. Kodama, Physica (Amsterdam) **320A**, 371 (2003).
[42] W. Weibull, J. Appl. Mech. (1951), https://hal.science/hal-03112318/document.
[43] S. Dash, B. K. Nandi, and P. Sett, Phys. Rev. D **93**, 114022 (2016).
[44] R. Chawla and M. Kaur, Adv. High Energy Phys. **2018**, 1 (2018).
[45] A. C. Bemmaor, Modeling the diffusion of new durable goods: Word-of-mouth effect versus consumer heterogeneity, in *Research Traditions in Marketing*, edited by G. Laurent, G. L. Lilien, and B. Pras (Springer Netherlands, Dordrecht, 1994), pp. 201–229.
[46] A. Singla and M. Kaur, Adv. High Energy Phys. **2020**, 1 (2020).
[47] R. Aggarwal and M. Kaur, Adv. High Energy Phys. **2020**, 1 (2020).
[48] R. Aggarwal and M. Kaur, Phys. Rev. D **102**, 054005 (2020).
[49] W. Weibull, ASME. J. Appl. Mech. **18**, 293 (1951).
[50] D. J. Mangeol, arXiv:hep-ex/0110029.
[51] D. Autiero *et al.*, Nucl. Phys. B, Proc. Suppl. **188**, 188 (2009).
[52] R. Acquafredda *et al.*, J. Instrum. **4**, P04018 (2009).

[53] H. Pirner, W. Chao, and M. Hegab, Nucl. Phys. **A399**, 515 (1983).
[54] A. J. Buras, J. D. De Deus, and R. Møller, Phys. Lett. **47B**, 251 (1973).
[55] D. Baranov *et al.*, Z. Phys. C **21**, 189 (1984).
[56] M. Praszalowicz, Phys. Lett. B **704**, 566 (2011).
[57] R. Sochorová, B. Tomášik, and M. Bleicher, Phys. Rev. C **98**, 064907 (2018).